
EFDA–JET–CP(07)03/46

E. Joffrin and JET EFDA contributors

Advanced Tokamak Scenario Developments for the Next Step

"This document is intended for publication in the open literature. It is made available on the understanding that it may not be further circulated and extracts or references may not be published prior to publication of the original when applicable, or without the consent of the Publications Officer, EFDA, Culham Science Centre, Abingdon, Oxon, OX14 3DB, UK."

"Enquiries about Copyright and reproduction should be addressed to the Publications Officer, EFDA, Culham Science Centre, Abingdon, Oxon, OX14 3DB, UK."

Advanced Tokamak Scenario Developments for the Next Step

E. Joffrin^{1,2}
and JET EFDA contributors*

¹*EFDA-JET-CSU, Culham Science Centre, Abingdon, Oxfordshire OX14 3DB, UK;*

²*Association EURATOM-CEA, DSM-DRFC, CEA Cadarache, 13108 St Paul lez Durance, France;*

** See annex of M.L. Watkins et al, "Overview of JET Results ",
(Proc. 2nd IAEA Fusion Energy Conference, Chengdu, China (2006)).*

Preprint of Paper to be submitted for publication in Proceedings of the
34th EPS Conference on Plasma Physics,
(Warsaw, Poland 2nd - 6th July 2007)

ABSTRACT

The objective of advanced tokamak scenario research is to provide a candidate plasma scenario for continuous operation in a fusion power plant. The optimisation of the self-generated non-inductive current by the bootstrap mechanism up to a level of 50% and above using high plasma pressure and improved confinement are the necessary conditions to achieve this goal. The two main candidate scenarios for continuous operation, the steady state scenario and long duration (up to 3000s) high neutron fluency scenario (the hybrid scenario), both face physics challenges in terms of confinement, stability, power exhaust and plasma control. Resistive Wall Modes (RWM) and Alfvénic fast ion driven instabilities are the main limitation for operating the steady state scenario at high pressure and low magnetic shear. In addition, this scenario demands a high degree of control over the plasma current and pressure profile and the steady state heat load on in-vessel plasma facing components. Understanding the confinement properties of hybrid scenario is still an outstanding issue as well as its modelling for ITER in particular with regard to the H-mode pedestal parameters. This scenario will also require active current profile control although less demanding than for the steady state scenario. To operate advanced tokamak scenario, broad current and pressure profile control appears as a necessary request to ITER actuators, in addition to the tools required for instability control such as error field coils or Electron Cyclotron (EC) current drive.

1. INTRODUCTION

In the period leading up to the recent decision on the construction of ITER, the programmes of existing tokamaks have strengthened the preparation of relevant plasma scenarios leading to the design definition of the systems required to operate those scenarios. Inductive operation of ITER relies on the so-called standard H-mode scenario (H for high confinement) [ITER physics basis, 1999] to demonstrate a fusion power amplification Q of 10 for typically 500s [Green 2003]. However inductive current drive uses a transformer, thus making this scenario inherently pulsed.

The work to develop different types of plasma scenario that could operate in steady state (i.e. non-inductively) at levels of fusion performance comparable to the conventional H-mode has become known as advanced tokamak research [Sips 2005]. In the past fifteen years tokamak programmes across the world have therefore devoted important technical and experimental efforts to the development of means to achieve steady state operation [Janeschitz 2005], [Kishimoto 2005], [Takanaga 2006], [Doyle & Wade 2006], [Sips 2002], [Litaudon 2007]. For this purpose external current drive systems are proposed for ITER [Bora 2007], [Jacquinot 2007] such as the injection of: electron cyclotron (EC) waves (105 to 170GHz); lower hybrid (LH) waves (3 to 5.7GHz); Ion Cyclotron (IC) waves (MHz); and Neutral Beam (NB) of high energy particles (up to 1MeV). However, the main component of the non-inductive current drive in advanced tokamak scenarios is actually provided by the plasma itself through the so-called bootstrap mechanism [Bickerton 1971] generated by the pressure gradients in the magnetic geometry of a tokamak. This “free” source of non-inductive current is maximised at high plasma pressure and low plasma current. On the other hand, the observation that energy

confinement degrades with decreasing plasma current provides the additional constraint that the energy confinement must be enhanced with respect to a standard H-mode scenario (i.e. $H > 1$, where H is the confinement time normalised to an established H-mode scaling). In this case, an equivalent fusion yield could be achieved with a plasma current smaller than would be necessary in H-mode. In addition, increasing the plasma pressure and reducing the plasma current can also change the Magneto-Hydro-Dynamic (MHD) behaviour of the plasma and instabilities can be encountered in these conditions that are otherwise not limiting in the standard H-mode scenario.

This paper is organised as follows: the first section develops, in more details, the motivations and key factors that have led to the steady state scenario concept and research and also defines the physical quantities used in the rest of the paper. Then examples of typical advanced scenarios so far developed in present devices are presented, namely the steady state non-inductive scenario for continuous operation and the so-called “hybrid” stationary scenario for long pulse operation (1000 to 3000 seconds in ITER). This more recent scenario uses a significant non-inductive current drive to provide longer pulse duration and high Q operation. In the third section, key physics and operational challenges for the advanced tokamak scenarios are introduced. These issues are important factors for ITER and the conclusions are directed towards defining technical requirements for steady state operation of ITER.

2. THE ADVANCED TOKAMAK CONCEPT

2.1. MOTIVATIONS

A tokamak uses a transformer such that the secondary current (the plasma current) is driven inductively by increasing continually the current in the primary circuit also called the Ohmic poloidal coils. This design effectively limits the pulse length to the time for the Ohmic coils to reach their maximum achievable currents. For this reason, the H-mode scenario is envisaged to operate for a duration not exceeding 500 seconds in ITER at a plasma current of 15MA [Green 2003]. Here a plasma scenario is defined as the sequence of operational events applied to the fusion device to prepare and then initiate the plasma, raise the plasma current to the required value, apply the auxiliary heating during the burning phase and finally extinguish the plasma discharge safely (figure 1). The H-mode scenario is characterised by a transition to a higher confinement state compared with L-mode (L for low confinement) produced by the presence of a layer of reduced transport at the plasma edge (also called the pedestal) when sufficient additional heating is applied on [Wagner 1984].

2.2. EXTERNAL CURRENT DRIVE REQUIREMENTS

The limited duration of inductive pulses could be a disadvantage for a future power-plant which has to generate electricity on a continuous basis. To achieve continuous (steady state) operation, the exclusive use of external driven current is however not an economic solution. The current drive efficiency ($\eta_{CD} = I_{CD} R n_e / P_{CD}$ where I_{CD} is the driven current, R the plasma major radius, P_{CD} the power injected by the current drive system, n_e the plasma density and R the plasma major radius) of NB and LH current drive systems is projected to be of the order of 0.3 to 0.4 1020MA/MW/m² in ITER. EC current drive

efficiency is more in the range of 0.2 to 0.1MA/MW/m² in the central half of the discharge. Therefore even with 33MW and 20MW of NB and EC power as planned in the ITER baseline start-up [Bora 2007], a maximum of 2.8MA of current drive can be produced in ITER (assuming $n_e = 10^{20} \text{ m}^{-3}$). Using an additional 20MW of LH current drive power (as is being considered) would raise this value to 4MA. At a lower density of $6 \times 10^{19} \text{ m}^{-3}$, this combination with LH current drive would generate 6.5MA non-inductive current. Such a current of 6.5MA would not support a plasma generating 500MW of fusion power and a fusion gain factor $Q = 6.8$ in this case (here, $Q = P_{\text{FUS}}/P_{\text{IN}}$ where P_{FUS} is the fusion power and P_{IN} the auxiliary input power).

The steady state scenario envisaged for ITER takes advantage, therefore, of the tokamak geometry and plasma pressure gradients to maximise the bootstrap current drive while maintaining sufficient confinement and stability to provide the necessary fusion yield.

2.3. BOOTSTRAP CURRENT

The bootstrap current in a tokamak is now a well considered and proven effect. First identified in 1971 [Bickerton 1971] [Galeev 1970], the evidence of the presence of bootstrap has been observed experimentally in several devices [Kikuchi 1995]. More recently a review [Peeters 2000] has discussed the specific role of this current to modify the total current profile for advanced tokamak scenarios.

The bootstrap current derives from the inhomogeneous toroidal field present in a tokamak (the toroidal field decays in the vacuum like $1/R$) creating a mirror which can trap plasma particles as they follow the magnetic field lines. In the presence of a radial pressure gradient in the plasma, adjacent trapped particle orbits provide a momentum imbalance that can be transferred to the passing particles by collisions. The bootstrap current is parallel to the magnetic field and by definition, requires the presence of trapped particles and a pressure gradient. For estimation purposes, the scalings of the bootstrap current with global plasma parameters have also been derived [Wilson 1992], [Hoang 1997], [Andrade 2006]. Typically the fraction of the plasma current driven by the bootstrap mechanism scales as: $I_{\text{boot}}/I_p = f_{\text{BS}} = C \cdot \epsilon^{1/2} \cdot \beta_p \sim C_{\text{BS}} \cdot \beta_N \cdot q_{95}$. Here $\beta_p = 2\mu_0 \langle p \rangle / \beta_p^2$ is the ratio of the volume averaged plasma pressure $\langle p \rangle$ to the poloidal magnetic field (β_p) pressure. $\beta_N = \beta_t [\%] \cdot a [\text{m}] \cdot B_T [\text{T}] / I_p [\text{MA}]$, where β_t is the averaged plasma pressure normalized to the toroidal field B_T : $\beta_t = 2\mu_0 \langle p \rangle / \beta_T^2$. C (~ 0.45) and C_{BS} are parameters depending weakly on current and pressure profile parameters. Many experiments across the world have demonstrated experimentally that a large bootstrap fraction can be achieved in a tokamak plasma by increasing the normalised pressure [Challis 1993], [Hobirk 2001], [Politzer 2005], [Takase 2007].

An important property of the bootstrap current is that it is not peaked in the plasma centre. Therefore, when maximized (at high plasma pressure and low poloidal field or plasma current) it is capable of changing the current profile shape and the toroidal magnetic field winding $q_{\text{cyl}} = r_{\text{BT}}/R B_p$ (where r is the minor radius coordinate) significantly from peaked to reversed in the plasma core. At high plasma pressure i.e. higher β_N , the current can become hollow and the q profile can change from monotonic (low at the plasma centre and high at the edge) to a case with an off-axis minimum q value (q_{min}) (figure

2). This creates a zone of negative magnetic shear s (where $s = r/q \, dq/dr$). With a moderate ratio of the plasma pressure to the current the q profile flattens in the plasma core giving a magnetic shear close to zero. Changing the magnetic shear in this way can have dramatic effects on the transport and stability properties of the discharge. The consequences on transport are briefly reviewed in the next section.

2.4. CONSEQUENCES OF THE BOOTSTRAP CURRENT ON CORE TRANSPORT

The role played by the details of the current profile shape in determining the transport properties of tokamak plasmas were intensively studied theoretically very early [Kadomtsev 1967]. Experimentally, a decrease in magnetic shear can be achieved by ramping up the plasma current while applying additional heating to delay the penetration to the plasma centre. Reduced energy and particle transport have been associated with a core region of negative (or reversed) magnetic shear in many experiments [Hugon 1992], [Litaudon 1996] [Bell 1998], [Wolf 2001], producing in this region a marked temperature and density peaking also called an internal transport barrier (ITB). Recently the dependence of the magnetic shear on electron heat transport was demonstrated experimentally in the TCV tokamak [Sauter 2006] (figure 3). This behavior is in line with theoretical predictions (see for example [Wakatani 1998], [Antonsen 1996]) showing the dependence of the growth rate of electrostatic potential fluctuations or ballooning-like radial structure on the magnetic shear as it is scanned from strongly positive to negative.

Another important factor thought to play a role in the stabilization of plasma turbulence is the shear in the plasma rotation. As with the effect of reversed magnetic shear, there is a substantial literature describing how ITBs can be produced through the stabilization of turbulence eddies by $E \times B$ sheared velocities [Terry 2000] [Hahm and Burrell 1995]. The most unstable long wavelength turbulent modes, the ion temperature gradient and trapped electron modes [Horton 1999] [Weiland 2000], can be stabilized linearly by an imposed external sheared flow (for example, through the injection of momentum) when the $E \times B$ flow shear exceeds the linear growth rate of these modes [Hahm and Burrell 1995] and produces an a layer with reduced transport (e.g. ITB) by turbulence stabilization [Beyer 2006]. Once an ITB is formed, a positive feedback loop can be established where the reduction in momentum due to the ITB transport (i.e. the pressure gradients) acts to increase the $E \times B$ shearing rate. It should be pointed out that this stabilizing mechanism is strongly dependent on the magnetic shear itself since the $E \times B$ shearing rate is also dependent on the magnetic field structure (i.e. on the magnetic shear s). These two effects are thus not independent.

The onset of an ITB or reduced transport through the reduction of the magnetic shear creates a feedback loop due to the bootstrap current. The increase of the latter (through the increase of pressure gradients) tends to reduce or reverse the magnetic shear further and so can amplify the pressure gradients changes. For the operation of steady state scenario, this important feedback mechanism implies that, for the operation of a steady state scenario, active control of the current profile will be required in order to maintain the scenario at a given operational point. This aspect will be discussed in further detail in section 4.3.

2.5. ROUTE TO CONTINUOUS TOKAMAK OPERATION

Given the above consideration, the advanced tokamak operation requires the optimisation of the fusion power while minimising at the same time the amount of power required to supply the current non-inductively. For stationary conditions with the ion temperature around 10keV, the fusion power can be estimated as:

$$P_{FUS} = C_{FUS} \langle p \rangle \tau_E H P_{LOSS} \propto C_{FUS} H \beta_N^2 / q_{95}^2 \quad (1)$$

where $P_{LOSS} \propto \langle p \rangle / H \tau_E$ is the plasma power exhausted from the plasma, τ_E the energy confinement time. Assuming steady state (i.e. fully non-inductive) and using the current drive efficiency hCD the non-inductive power P_{CD} can be written as [Luce 2005]:

$$P_{CD} \propto (1 - C_{BS} / q_{95}) \cdot f_G = \frac{B_T}{C_{CD} q_9} \quad (2)$$

where f_G is the density normalised to the Greenwald value: $f_G = \pi a^2 n / I_p$ (where a is the minor radius at the plasma boundary in meter, n expressed in unit of 10^{20} m^{-3} and I_p in MA). It can be seen from expressions (1) and (2), that the fusion power P_{FUS} is maximised and the current drive power P_{CD} minimised when β_N is maximized. In addition, increasing q_{95} is very efficient for minimizing P_{CD} but also reduces P_{FUS} by a similar amount. In expression (1), this could be compensated if the H factor could be increased significantly above unity.

To summarise this section, the advanced tokamak scenario defines a mode of operation for a tokamak where a large fraction of plasma current is driven non-inductively with a large fraction (>50%) provided by the self-generated bootstrap current. At the same time, improved confinement ($H > 1$) is required to compensate for the lower plasma current (i.e. higher q_{95}) and reach Q above 5 as envisaged for the ITER steady state demonstration. By varying the q profile shape through the pressure increase (i.e. through the bootstrap current) or other external current drive means, a large variety of plasma scenarios can be obtained with different stability and transport properties. Consequently, advanced tokamak research has so far resulted in the development of several alternative approaches all using the bootstrap current as a tool to extend the discharge duration and modify the properties of the discharge with respect to the standard H-mode scenario. Experiments have focused on the development of the two scenarios introduced above: the non-inductive scenario for continuous operation and the hybrid stationary scenario for long pulse (up to 3000 seconds in ITER) and high neutron fluency. These specific scenarios are now described in the next section.

3. EXAMPLES OF ADVANCED SCENARIO DEVELOPMENT

3.1. STEADY STATE SCENARIO.

In the envisaged steady state non-inductive operation of ITER scenario [Green 2003], the plasma current during the current flat top phase is generated non-inductively by external current drive (such as LH, EC and NB) with a large fraction of bootstrap current (approximately 50%). The plasma current would be

9MA with a broad q profile with low magnetic shear (close to zero) in the plasma core. This scenario would have the following parameters: $q_{95} = 5$, $\beta_N \sim 2.9$, $H > 1.6$ and $f_G \sim 0.8$ and would produce typically 350MW of fusion power, resulting in a fusion gain factor of $Q = 5$ [Green 2003].

Figure 4 shows a prototype of a steady-state scenario run in the DIII-D tokamak with $I_p = 1\text{MA}$, $q_{95} = 5$ and a density close to 30% of the Greenwald value [Murakami 2006]. The q profile was flat in the plasma core with $q_{\text{min}} \sim 1.7$. The non-inductive current is close to 100% with a bootstrap current contribution of 60%, 30% of NB current drive and 8% of EC current drive located at about $r/a = 0.4$. The normalised pressure reaches $\beta_N = 3.4$ and the H factor was above unity ($H \sim 1.4$) making this scenario relevant in many respects to the steady state ITER targets for reaching $Q = 5$. The increased H factor could be explained by the broadly elevated ion temperature at $r/a < 0.6$ possibly due to ExB shear substantially reducing ion temperature gradient turbulence. Steady state scenarios are also currently developed in other devices such as JET [Challis 2007], [Litaudon 2007] or JT-60U [Sakamoto 2006].

3.2. “HYBRID” SCENARIO

In this more recently developed mode of operation, the external current drive systems and the bootstrap current provide a substantial fraction ($\sim 50\%$), but not all, of the total current. The burn time in ITER would be significantly increased with respect to the dominantly inductive H-mode scenario to reach up to 3000s. For this regime, the value of q in the plasma core would be in the range 1.0- 1.5 with the magnetic shear close to zero. The benefit of the slightly raised central q value compared with a standard H-mode is the avoidance of significant sawtooth activity that can trigger deleterious tearing mode instability (so-called neoclassical tearing modes [Guenter 2003]) in standard H-mode plasmas. In ITER, this scenario would be operated at slightly lower plasma current ($I_p \sim 13\text{MA}$) and $q_{95} = 4$, $\beta_N \sim 2.0-2.3$ and $H \sim 1.0$ and $f_G = 0.85$ to produce a $Q = 5$ and 350MW to 500MW of fusion power for 1000 to 1600 seconds [Green 2003].

An example of a typical hybrid scenario run in the ASDEX Upgrade tokamak with $I_p = 1\text{MA}$, $q_{95} = 3.8$, and moderate density ($f_G \sim 0.4$) is shown in figure 5 [Staebler 2005]. Please note that in publications from ASDEX Upgrade, the hybrid scenario is often referred to as “improved H-mode”. In ASDEX Upgrade, the q profile was preformed to provide q greater or close to unity by early NBI heating starting 0.3 seconds after plasma initiation, during the current ramp phase in order to reduce the current diffusion by increasing the electron temperature. The NBI power was stepped up to 5MW at the beginning of the current flat-top ($t = 1\text{ s}$), which immediately leads to the formation of an H-mode scenario. In the example shown in figure 5, the NBI power was increased to almost 10MW in two successive power ramps. After the first ramp, β_N rose to a value close to 3. At the same time, the H-factor increased with the increasing input power from $H = 1.1$ to 1.4 during the high β_N phase. Such behaviour has often been observed in hybrid scenario discharges in this device. No sawteeth were observed during this phase but at 4.9s a small amplitude (3, 2) tearing mode developed, which affected the confinement only slightly. In this discharge about 30% of the current was driven non-inductively by the bootstrap mechanism and by the beam driven current. Scenarios of this type have been run

routinely in ASDEX Upgrade, JET [Joffrin 2005], DIII-D [Wade 2005] and JT-60U [Oyama 2006] with performance in close agreement with the ITER target [Imbeaux 2005].

As will be discussed in next section, hybrid scenario experiments [Sips 2002] in ASDEX Upgrade and also in DIII-D [Wade 2005] have found an H factor greater than unity. This suggests that this scenario could have the potential to increase its fusion gain. However, as indicated above, ITER performance assessments are assuming H=1 in all their simulations.

4. KEY PHYSICS ISSUES FOR STEADY STATE AND HYBRID SCENARIOS

4.1. CONFINEMENT AND TRANSPORT

The standard H-mode scenario confinement scaling law IPB98(y,2) [ITER physics basis 2007] has been derived on the basis of a large database from 18 different tokamaks of different sizes and plasma shape and can be expressed in terms of dimensionless parameters as:

$$B \tau \sim \rho^{*-2.70} \beta^{-0.90} \nu^{*-0.01} q^{-3.0} e^{0.73} k^{3.3}$$

Where ρ^* is the normalised Larmor radius, ν^* the normalised collisionality, $\epsilon = a/R$ and k the elongation. This scaling provides a basis for estimating the energy confinement properties of next step devices such as ITER. Most of the 3762 discharges used to derive this scaling are H-mode scenarios. So the question arises as to whether such a scaling applies to advanced tokamak scenarios, which can operate in a different range of parameters in particular at higher normalised pressure. Global performance analyses have shown that the ITER operational space is indeed sensitive to the b dependence of the confinement scaling used in the extrapolation from present devices. Given the strong negative dependence of the present IPB98(y,2) scaling with b , confinement extrapolation for advanced tokamak scenarios is particularly affected.

It is then interesting to review the parameter space covered by database in terms of β and ρ^* [McDonald 2007]. Figure 6 presents the extent of the H-mode database in the β_N - ρ^* space at low ITER relevant ρ^* . It can be seen that the present database, does not cover high values of β where the advanced tokamak scenario would be expected to operate. This lack of data at high normalised pressure introduces an uncertainty when one uses the confinement scaling to extrapolate the performance of advanced tokamak scenarios to the ITER values of ρ^* and β .

With the development of advanced tokamak scenarios and in particular with the stationary hybrid scenario developments, new data have been produced at higher normalised pressure (up to $\beta_N = 3.2$) than those in the present H-mode database. In the hybrid scenario, DIII-D has shown a confinement improvement factor up to 1.6-1.7 [Wade 2005 & Luce 2005]. The ASDEX upgrade hybrid scenario also shows improved confinement with a factor up to 1.4-1.5 [Sips 2007]. However, JET does not observe improved confinement with respect to the H-mode scaling. This difference could be due to the lower values of thermal normalised pressure range in JET experiments (not exceeding 2.2 compared with 3.2 in ASDEX Upgrade and 2.7 in DIII-D). It is possible that different q profiles or $E \times B$ shearing

rates are produced in the last two devices, thus creating improved transport conditions. The b dependence of confinement in the H-mode scenario (i.e. at bN around 2) has been investigated in all three devices [McDonald 2003] [Vermare 2007] [Petty 1998]. However, no firm conclusion on the b dependence has yet been drawn. Nevertheless, it is certain that the increase of the hybrid scenario database does provide the possibility to further refine the confinement scaling and extend the β_N - ρ^* space so that the b dependence can be better understood. This issue is crucial for the extrapolation of the advanced tokamak scenarios towards ITER.

The contribution of the H-mode edge pedestal to the global confinement has been investigated in advanced tokamak scenarios and compared with that of the H-mode scenario. The scaling of the pedestal energy for the H-mode scenario has been inferred from the above multi-machine database mentioned above [McDonald 2007]. Experimental analyses of advanced tokamak discharges have not shown any clear difference in the pedestal confinement with respect to the H-mode in JT-60U [Kamada 2006], in contrast to ASDEX Upgrade where the confinement improvement seems to originate from the pedestal in the hybrid scenario [Maggi 2007] and DIII-D where this appears to originate from the core [Maggi 2007, Groebner 2006]. The prediction of advanced tokamak scenario performance for ITER by modelling uses the pedestal temperature as a boundary condition and is therefore very dependent on pedestal parameters such as the pedestal temperature. Figure 7 shows the sensitivity of the ITER performance in the hybrid scenario predicted using the GLF23 transport model to the edge temperature assumed at the top of the H-mode edge pedestal [Kessel 2005]. It is apparent that core confinement uncertainties make a minor contribution to the global confinement and plasma performance in this modelling compared with the prediction of the pedestal parameters. A substantial effort [Connor & Wilson 2000] has been devoted to this question, but so far, the variety of pedestal observations cannot be encompassed by a single theoretical framework. The other related issue here is the dependence of the edge bootstrap current generated on the pedestal gradient at the pedestal. In the absence of a reliable prediction of the edge pressure gradients, and thus of the bootstrap current, it is also difficult to confidently infer the value and evolution of the current density in the plasma core. The three cases marked by a point on figure 7 show the variation in q stationary profile as the pedestal temperature or the input power is varied (different values of the central q value q_0 and the radius of the $q=1$ surface are shown). The H-mode edge pedestal has also a large impact on the modelling of the q profile in hybrid scenarios. This is a crucial issue for the determination of the current drive sources required to maintain the optimum q profile (i.e. with q close to or above unity) in ITER.

As described in section 2.4, internal transport barriers provide an interesting tool to simultaneously improve the confinement and increase the bootstrap current in advanced tokamak scenarios. In this respect, it is a very attractive feature for achieving steady state operation. Many experimental studies and reviews have examined the origin, physics and potential use of internal transport barriers [Connor 2004] [Wolf 2002] [Challis 2004] [Litaudon 2006]. What follows, is a discussion of just two of the key operational issues related to ITBs. The first relates to the so-called bootstrap alignment and the

second to impurity accumulation and particle transport in ITB plasmas.

ITB formation is closely linked to the details of the q profile shape and in particular to plasma regions with zero magnetic shear point and to low order rational q surfaces [Joffrin 2003, Austin 2006]. But there is so far no evidence that the maximum bootstrap current (i.e. located at the maximum plasma pressure gradient) is naturally aligned with the position of the minimum of the q profile, which would be a necessary condition for sustaining the q profile in steady state conditions. Some experimental evidence in JT-60U [Takase 2006] suggests that the outer edge of the ITB is located at the same position as q_{\min} or at a low order rational q surface in the negative region. In this case, the bootstrap current would peak inside the q_{\min} location and hence, expected to reduce the shear reversal of the current profile. This potential problem may be less severe for scenarios where an ITB is located in the positive magnetic shear region of the plasma as in this case the pressure gradients would be better aligned with the minimum q value. Nevertheless, some external driven current is likely to be needed in either scenario to maintain the q profile required for the sustainment of the ITB in stationary conditions. Experiments in JT-60U [Fujita 2002], Oikawa [2000] have managed to operate stable ITBs at high pressure by finding the appropriate bootstrap current and external non-inductive current combination. However, so far it is not clear yet how much power is required to achieve this in ITER. On the other hand, it is expected that the externally driven current would be required at relatively large plasma radius ($r/a > 0.7$) in order to sustain a wide ITB encompassing at least half of the plasma volume in order to maximise the resulting confinement enhancement.

The second issue relating to steady state ITBs, is the behaviour of particle transport in such plasma. Several experiments [Dux, 2003] [Takenaga, 2003] [Giroud 2005] [Burrell 2003], have demonstrated that impurities such as neon, argon, carbon, helium and even deuterium accumulate inside the ITB region. The particle confinement appears to correlate with the normalised temperature gradient strength (fig.8), which is a measure of the energy transport reduction caused by the ITB. This observation would be consistent with a strong inward convection velocity for all species at the ITB. There is also evidence that the particle transport inside the ITB depends on the magnetic shear through the curvature pinch as described in the following review on transport physics: [Garbet 2004]. In JT-60U [Takenaga 2005], EC heating has been tried as a tool to increase the turbulent transport inside the ITB and thus degrade particle transport for driving impurities out of the ITB. ASDEX Upgrade has reported results showing, in particular the control of the tungsten concentration in the core of H-mode discharges [Neu 2006]. Also, there is some evidence that maintaining the temperature gradient of the ITB and the degree of shear reversal of the q profile to moderate values also can help to prevent impurities accumulation. It should be noted here that in the context of a burning plasma the alpha particle heating might be expected to provide a centrally peaked electron power deposition profile favorable for impurity transport.

To provide the required improvement in the confinement of advanced tokamak scenario, there appear to be a significant advantage in the use of moderate ITBs at large plasma radius, whilst being optimised in terms of bootstrap current alignment and impurity accumulation.

4.2. STABILITY

The modification of the q profile has the effect of substantially changing the stability conditions of the advanced tokamak plasmas. In the hybrid scenario, the increase in q in the plasma core by the off-axis non-inductive current drive results in a reduction of the size of the $q=1$ surface size which is responsible for the sawtooth instability. In high normalised pressure scenarios, sawteeth can trigger by non-linear toroidal coupling topological rearrangements of the magnetic field lines through magnetic reconnection also called Neoclassical Tearing Modes (NTM) [Guenter 2003]. The reduction or elimination of sawteeth prevents this coupling and has a beneficial effect on stability in hybrid scenario. However, in the hybrid scenario, $m=2$ $n=1$ modes and $m=3$ $n=2$ NTM mode activity can still be observed [Wade 2005] [Staebler 2005] [Joffrin 2005]. The first is generally the most deleterious one as it can lead sometimes to a disruption. The second mode is often present in hybrid regimes but only causes a degradation of the confinement of 10% to 15% when its radial extent reaches 1/10 of the minor radius in size. In both cases techniques have been developed in ASDEX Upgrade [Maraschek 2005], DIII-D [Prater 2006] and JT-60 [Isayama 2006] to control actively the island size using localised EC current drive in the O-point of the island to replace the missing bootstrap current that destabilises the island. In the latter case, an active control method has been developed to control both the 2/1 and the 3/2 islands using steerable mirrors to control the power deposition profile of the EC current drive waves and tracking the island location. This strongly suggests that q profile control will be required in the hybrid scenario both to stabilise NTMs and to prevent the onset of sawtooth instabilities by controlling the $q=1$ surface. It should be pointed out here that in JET the onset of the $m=2$, $n=1$ mode is rarely observed in the hybrid scenario [Buttery 2007]. This difference might be due to factors such as the machine size or differences in the q profile shape, but further analysis is required to identify the underlying cause.

In the case of the reversed shear q profile and high pressure commonly present in the steady state scenario, the plasma is subject to ideal pressure driven $n=1$ kink MHD instabilities. Due to its ideal nature, this activity can grow very quickly with the Alfvén time ($\sim 10^{-7}$ s) when it exceeds the so-called “no-wall” β limit. However the conducting wall of a tokamak provides a stabilising effect by the mirror currents generated within it and the mode continues to grow with the time scale of the vessel skin time (generally a few milliseconds) thus allowing access to higher pressure. In addition, the misalignment of the tokamak coils can produce an intrinsic error of the radial magnetic field. Plasmas operating above the no-wall limit tend to amplify this error field. It has been found that plasma induced rotation by neutral beams [Strait 2007] and the correction of the intrinsic error field by external coils [Okayabashi 2006] are two possible ways to stabilise these modes above the no-wall limit. One of these techniques is routinely used in DIII-D in their steady state scenario experiments where the mode suppression is achieved by active control of the error field correction using measurements of the mode growth. In ITER, preliminary estimation indicates that the rotation created by the 1 MeV beams would be sufficient to stabilise resistive wall modes [Oikawa 2007]. In JET, the “no-wall” limit has been determined experimentally using external error field correction

coils as a diagnostic. An imposed oscillating (10 to 20Hz) error field is created by the coils and the plasma response was recorded during the high b phase of advanced tokamak scenario experiments. When the pressure exceeded the “no-wall” limit this imposed error is amplified so that the moment when the limit is exceeded can be determined [Gryaznevitch 2007]. This experimental technique has been applied to a large number of discharges where the q profile has been scanned from $q_{\min} > 2$ to $q_{\min} \sim 1$ while keeping the edge q identical (i.e. at the same plasma current) [Challis 2007]. The normalised pressure achieved at the time of the error field amplification is shown in figure 9 as a function of the time when the NB power has been applied. The neutral beam timing is a signature of q_{\min} during the main heating phase: when the NBI timing is advanced in the current ramp up, the current density profile penetration is stopped earlier at a higher q_{\min} value. This experiment illustrates the sensitivity of the “no-wall” limit to the q profile. The actual limit in the presence of a conducting wall has been also estimated from the DCON code [Glasser 1997] and is typically 30% higher than the no-wall limit. More experiments of this type are required to identify the dependence of the no-wall limit with the detailed shape of the q profile and other aspects of the plasma configuration [Turnbull 1998] to be able to operate the advanced tokamak scenario reliably and significantly above the no-wall limit and increase its performance. It should be noted that broad current density and pressure profiles are thought more favourable for RWM stability [Bondeson 1999]. This gives another incentive for operating advanced tokamak scenarios with a large radius ITB and broad current density profile. Nevertheless, the control of RWM could provide greater margins in normalised pressure to expand the operating domain of the steady state scenario. In ITER, this suggests that error field correction coils and possibly rotation control would be a valuable asset in the machine capability to achieve steady state at high β_N .

In a burning advanced tokamak scenario plasma, fast particle driven instabilities are likely to become a key issue. Energetic alpha particles are expected to transfer their energy by collisions to the thermal plasma and provide central electron plasma self-heating. These fast ions at a few MeV are close to the Alfvén speed and can resonate with magnetic field lines and therefore be lost by fluctuations in the Alfvén mode frequency range. Evidence of rapid transport has already been reported in several devices [Testa 2002] [Shinohara 2004] and simulation studies indicate that energetic ion redistribution takes place because of these Alfvénic modes [Zonca 2002] [Vlad 2006]. An important property of these modes is their sensitivity to the q profile shape. Therefore, the prediction and experimental confirmation of their presence and role in the steady state scenario and hybrid scenario is crucial for the validation of these scenarios for ITER. Recently, the stability of Alfvénic instabilities has been simulated for these two scenarios using the MHD-gyrokinetic code (HMGC) [Vlad 2006]. This calculation includes also the most relevant damping mechanisms for these modes such as the ion and trapped electron Landau damping. Figure 10 shows the growth rate of the Alfvénic instabilities in both hybrid and steady-state scenario for different modes as a function of the fast ion central pressure. It appears that the modes are more unstable for the steady state than for the hybrid scenario confirming that the q profile shape plays a significant role. As a consequence,

the fast ions losses are also different in the two scenarios. Typically the steady state scenario would be expected to lose 3% of its fast ion population, i.e. about 2MW of the alpha power. For the hybrid scenario, no significant loss of fast particle is predicted. If the fast ion pressure were doubled then the loss would be increased to ~10% (i.e. 8MW) and less than 1% (i.e. ~1MW) respectively. It is necessary to validate these estimations experimentally, since they do not consider all possible damping processes. However, they already suggest that fast particle losses could become a challenge particularly for the steady state scenario due to the potential losses to the first wall of the vacuum chamber.

4.3. PROFILE CONTROL AND EXHAUST

As mentioned earlier, active control is an essential requirement for the operation of advanced scenarios [Joffrin 2003] [Humphreys 2006]. Examples have already been provided in the previous section for the control of NTMs with EC current drive and RWM using error field coils. More importantly the feedback loop between the pressure and the current profile at high b_{N-} illustrates the need to develop profile control techniques to establish and sustain the scenario. A difficulty that has been identified is the different time scales for the evolution of the q and pressure profiles. Without significant MHD activity, the first evolves with the resistive time scale (typically ~100s in ITER) and the second with the confinement time (~3s in ITER). This means that the response of the control loop cannot be of the same time-scale for both quantities. The second challenge is the highly non-linear character of an ITB when it is created. There is in general no method to take into account such non-linearities in the design of a controller. As a result, existing controllers have been built on the basis of a linear response models around the target state to be controlled. Using this principle, successful experiments have been carried out to control the q profile together with the plasma temperature gradient in JET using three actuators (namely ICRH, NBI, and LHCD) [Mazon 2003]. Also, ITB active control has been achieved in JT-60U with the LH current drive [Suzuki 2006] and current profile control with EC current drive in the current ramp-up in DIII-D [Ferron 2006]. In addition, a two-time scale model for current and pressure control has been developed in JET to perform profile control experiments [Moreau 2006] [Laborde 2005]. In the future, it is necessary to validate this procedure in plasmas with high normalised pressure and, due to the uncertainties in transport models [Tala 2005], determine the appropriate control matrix by dedicated open loop experiments.

The development of plasma profile control techniques is likely to provide new requirements for the actuators on ITER in particular the current drive and heating systems. For example, current drive systems such as NB will require a variable power control capability to provide profile feedback control [Oikawa 2007]. Neutral beam injection is also an important actuator to deliver either rotation for the stabilisation of RWM or to drive current in on- or off-axis locations. Both the beam energy and geometry of the neutral beam system are important parameters. Moreover, there are indications that LH current drive would be an important actuator for driving a current at large plasma radius (at $r/a=0.7$) since its current drive efficiency is significantly larger than for EC current drive at this

location. Together with the neutral beams, LH current drive can play an important role in the control of the current profile broadening. Since there are still significant uncertainties in the modelling of the advanced tokamak scenarios it is important to ensure a high degree of flexibility in the design of these systems, compatible with their technical and engineering requirements.

When using current drive heating system as actuators, the control has also to be compatible with other limits such as heat loads on vessel components. For instance, fast electrons generated in the fields near the LH-launcher can produce highly localised heating in location magnetically connected to the antenna [Mailloux 1997] [Goniche 2006]. The Tore Supra experience with long pulses operation has demonstrated that active control of local heat loads can be achieved in combination with profile control [Joffrin 2006] by modulating the output power of the antenna.

The use of current drive and heating systems up to a level of 73MW (20MW ECCD + 20MW LHCD + 33MW NBCD) in ITER [Bora 2007] at lower density than in the standard H-mode scenario (typically $6-7 \cdot 10^{19} \text{ m}^{-3}$ line averaged, instead of $11-12 \cdot 10^{19} \text{ m}^{-3}$) also places more severe constraints on the steady state power exhaust. In the advanced scenario more than 100MW of loss power will cross the separatrix. In ITER, the required minimum density at the separatrix is predicted to be at least $3.3 \cdot 10^{19} \text{ m}^{-3}$ in the standard H-mode scenario in order to achieve acceptable power load on the divertor target ($< 10 \text{ MW/m}^2$) [Janeschitz 2000]. In an X-point magnetic configuration, this power is generally conducted through the scrape off layer down to the target plate where it is convected by elastic and charge exchange collisions. Because of the dependence of their cross-section on temperature, these physical processes are optimum for a sufficiently low temperature of 5eV [Stangeby 2000]. For a lower core density, the edge density is decreased and the temperature in the scrape-off layer higher. This leads to a much higher temperature that lowers the momentum loss by charge exchange collisions at the divertor targets. Seeding the plasma in the divertor region with impurities that dissipate a significant fraction of the conducted power by radiation before it can reach the divertor targets, could mitigate this problem. Experiments have explored this possibility in the hybrid scenario using nitrogen, argon or neon [Corre 2007], [Petrie 2006] [Takenaga 2005] and also in the steady state scenario [Litaudon 2007]. A key question here is whether it is possible to radiate the power without contaminating the plasma with the seeding impurity. This is possible if the ionisation length (mean distance travelled by a neutral particle before being ionised) of the impurity is short enough for it not to penetrate the plasma. Otherwise it can be ionised inside the H-mode pedestal where it can affect the performance of the core plasma. Recent JET experiment suggests that nitrogen is effective for radiating in the conducted zone of the scrape-off without contaminating the plasma dramatically [Corre 2007].

Other solutions have successfully mitigated the steady state heat load on the divertor targets by sweeping the strike point over the divertor target plates [Villone 2007]. Nevertheless, operation with stable plasma edge conditions, compatible with target heat load that satisfy engineering limits, remains a significant challenge for future advanced tokamak scenarios experiments

5. ADVANCED TOKAMAK SCENARIO REQUIREMENTS FOR ITER AND CONCLUSIONS

In this paper, the motivations for the advanced tokamak concept have been stated and two such scenarios have been discussed in detail: the steady state non-inductive scenario and the hybrid stationary scenario. Important issues in the design of an advanced tokamak scenario have been reviewed and the importance of operating these scenarios at high plasma pressure close to the stability limits has also been stressed.

Considerable progress has already been made and advanced scenarios have been recently operated on several devices (JET, JT-60, ASDEX Upgrade and DIII-D) for time scales of the order of the current diffusion time [Mikkelsen 1989] and with parameters relevant to ITER. Key physics issues related to the advanced tokamak are still being investigated and have been discussed in this paper. They indicate some of the main areas of research that are required for the further development of the advanced tokamak scenarios and their validation for ITER. These points include:

- There is an outstanding confinement issue regarding the scaling of energy confinement with β for advanced tokamak scenarios.
- The sensitivity of the prediction of fusion power and current density profile to the presently uncertain extrapolation of the pedestal parameters and structure.
- If ITBs are to be used for confinement improvement, broad current profile and ITB ($r/a > 0.7$) with moderate temperature gradient to avoid impurity accumulation and instability at high pressure has to be demonstrated.
- The importance of NTM control has been demonstrated with ECCD in the hybrid scenario. However, there is uncertainty concerning the role of the 2/1 NTM as it is not limiting in JET as in other machines.
- The control of RWMs for steady state scenarios has been demonstrated in DIII-D. The optimisation of the q profile and plasma shape for operation beyond the no-wall limit remains an issue for the optimisation of this scenario.
- The role of Alfvénic modes that appear to be more unstable in the steady state scenarios than in the hybrid scenario from simulation. The role of the q profile on the Alfvénic modes remain to be validated experimentally.
- The handling of the steady state exhaust power loss in advanced tokamak scenario is an issue. Further edge characterisation and the development of techniques to mitigate the temperature on the divertor target and on plasma facing components is necessary.
- Finally the control of the pressure and q profile is still a challenging issue but remains a necessary objective. However, profile control techniques have not yet demonstrated their potential at high normalised pressure.

As discussed in the paper, advanced tokamak developments have already identified essential technical requirements for establishing long pulse or continuous operation in ITER.

The table below summarizes the technical requirements and their potential functions for advanced tokamak operation:

Systems	Function	Status in ITER [Bora 2007]
<i>Error field coils</i>	<i>RWM stabilisation</i>	<i>Considered</i>
LHCD	Current drive at large plasma radius ($r/a \sim 0.7$) for control of broad current control operation.	Considered: 20-40MW, Frequency: 5GHz
NBCD	On- or near-axis current drive ($r/a \sim 0.3$) and plasma rotation for RWM stabilisation and shear plasma flow	33MW planned. 50MW considered. Beam Energy: 1MeV
ECCD	On- or off-axis current drive ($r/a \sim 0.5$) 2/1 & 3/2 NTM and sawteeth control and core impurity control	20MW planned, 40MW considered. Frequency: 170GHz
ICCD	On-axis current drive for central q control. Low current drive efficiency [ITER physics basis, 2000].	20MW planned, 40MW considered. Frequency: 23-56MHz

Given the uncertainties in the modelling of advanced tokamak scenarios, it is not yet possible to provide precise requirements for the heating systems and it is possible that the different scenarios considered here may give rise to different and perhaps conflicting specifications in the future. However, the need for control of broad current density profile for both improved confinement and stability reasons appears to emphasize the role of lower hybrid current drive in ITER for both the steady state and hybrid scenarios. NB and EC current drive also appear essential for the operation of the hybrid scenario.

In conclusion, progress in advanced tokamak research has been considerable in the past fifteen years. Many technical and physics issues have been addressed in depth and are still being investigated. This research has led to the understanding of the importance of integrated operation and validation of the candidate scenarios for steady state or long pulse operation. With the coming of ITER, this research is now in a stage where it has to provide specifications for the actuator systems and define the operational margins for the advanced tokamak scenario. This task is essential in view of delivering to a fusion power plant an option for continuous operation [Galambos 1995].

ACKNOWLEDGEMENT

The author would like to thank most particularly the specific contribution for the material used in this paper from Drs J.F. Artaud, M. Gryaznevitch, C. Kessel, D.C. McDonald and G. Vlad. The author is also very grateful C. Challis, J. Hobirk, R. Kamendje and A.C.C. Sips for the careful reading of the manuscript. The many discussions the author had with the following persons to accomplish this work are also gratefully acknowledged: A. Becoulet, P. Beyer, D. Borba, R. Buttery, J. de Boo, P. de Vries, R. Felton, W. Fundamenski, C. Giroud, S. Ide, J. Jacquinot, A. Klein, A. Loarte, T. Luce, X. Litaudon, J. Menard, J. Ongena, D. Testa.

REFERENCE

- Andrade M. C. R. et al., 33rd EPS Conference on Plasma Phys. Rome, 19 - 23 June 2006 ECA Vol.**30I**, P-1.189 (2006)
- Antonsen T.M. et al., Phys. Plasma **3** (1996) 2221
- Austin M. et al., 21st Fusion Energy Conference, 16-21 October 2006, Chengdu, China, EX/P3-1
- Baisuk V. et al, Nuc. Fusion 43 (2003) 822-830
- Bell M G et al 1999 *Plasma Phys. Control. Fusion* **41** A719-A731
- Beyer P. et al., Plasma Phys. Control. Fusion **49** (2007) 507-523
- Bickerton R. J. et al. 1971 Nat. Phys. Sci. **229** 110
- Bondeson A. et al., Nucl Fusion **39** (1999) 1523
- Bora D., 17th Topical Conference on RF power in Plasmas, 7 May, 2007
- Burrell K H 1999 Phys. Plasmas **6** 4418
- Burrell K H Nucl. Fusion **43** (2003) 1555-1569
- Buttery R.B. et al., this conference
- Challis C. D. et al., this conference
- Challis C. D., Plasma Phys. Control. Fusion **46** (2004) B23-B40
- Challis C.D. et al 1993 *Nucl. Fusion* **33** 1097-105
- Connor J. W. et al., Nucl Fusion **44** (2004) R1-R49
- Connor J.W. and Wilson H.R. *Plasma Phys. Control. Fusion* **42** (2000) R1
- Corre Y. et al., this 2007 conference
- Doyle E. J. Plasma Phys. Control Fusion **48** (2006) B39-B52
- Dux R. et al. *Nucl. Fusion* **44** No 2 (February 2004) 260-264
- Ferron J. et al., *Nucl. Fusion* **46** No 10 (October 2006) L13-L17
- Fujita T. et al., Plasma Phys. Control. Fusion **44** (2002) A19-A35
- Galambos J. D. et al., Nuc. Fus. **35** (1995) 551
- Galeev A. A., Zh. Eksp. Teor. Fiz. **59**, 1378 (1970)
- Garbet X. et al., Plasma Phys. Control. Fusion **46** (2004) B557-B574
- Giroud C. et al. *Nucl. Fusion* **47** No 4 (April 2007) 313-330
- Goniche M. et al., 21st Fusion Energy Conference, 16-21 October 2006, Chengdu, China, EX/P6-12.
- Glasser A. H., The direct criterion of Newcomb (DCON) for the stability of an axisymmetric toroidal plasma, Los Alamos Report No. LA-UR-95-528, 1997.
- Green B. J., Plasma Phys. Control Fusion **45** (2003) 687-706
- Greenfield C. M. Plasma Phys. Control. Fusion **46** (2004) B213-B233
- Groebner R. J. et al., Plasma Phys. Control. Fusion. **48** (2006) A109-A119
- Gryaznevitch et al., 2007 this conference
- Guenter S. et al., Nucl. Fusion **43** No 3 (March 2003) 161-167
- Hahm T S and Burrell K H 1995 Phys. Plasmas **2** 1648

Hoang G.T., et al. Proc. of the 24th EPS Conference, **vol.21A**, part III, p.965, Berschtesgaden, Germany (1997).

Hobirk J. et al., Physical Review Letters **87**(8), (2001) 085002-1-085002-4

Horton W., Rev. Mod. Phys. **71** (1999) 735

Humphreys D. et al., 21st Fusion Energy Conference, 16-21 October 2006, Chengdu, China, IT/2.6

Hugon M. et al., Nucl. Fusion **32** (1992) 33

Imbeaux F. et al., Plasma Phys. Control. Fusion **47** (2005) B179-B194

Isayama A. et al., *Plasma Sci. Technol.* **8** No 1 (January 2006) 36-40

ITER physics basis, Nuc. Fus. **39** (1999) 2137-2638

ITER physics basis, Nucl. Fusion **40** No 7 (July 2000) 1429

Jacquinet J., 17th Topical Conference on RF power in Plasmas, 7 May, 2007

Janechitz et al., Nuc. Fus. **40** (2000) 1197

Joffrin E. et al., 21st Fusion Energy Conference, 16-21 October 2006, Chengdu, China, EX/1-6, submitted to Nuc. Fus. 2007.

Joffrin E. et al., Nucl. Fusion **45** (2005) 626-634

Joffrin E. et al., *Plasma Phys. Control. Fusion* **45** No 12A (December 2003) A367-A383

Joffrin E. et al., Nucl. Fusion **43** (2003) 1167

Kadomtsev B. B. and Pogutse O. P. Sov. Phys. JETP **24** 1172

Kamada et al., Plasma Phys. Control. Fusion **48** (2006) A419-A427

Kessel C. et al., 21st IEEE/NPSS Symposium on Fusion Engineering, 2005, Knoxville, Tennessee, USA, 1-4244-0150-X/06

Kikuchi M and Azumi M, Plasma Phys. Control Fusion **37** 1215

Kikuchi M. and the JT-60 Team, Plasma Phys. Control. Fusion **43** (2001) A217-A228

Kishimoto H. et al., Nucl. Fusion **45** (2005) 986-1023

Laborde L. et al., *Plasma Phys. Control. Fusion* **47** No 1 (January 2005) 155-183

Litaudon X et al 1996 Plasma Phys. Control. Fusion **38** 1603

Litaudon X. et al., Plasma Phys. Control Fusion **48** (2006) A1-A34

Litaudon X., This EPS 2007 conference

Luce T. C. et al., Nucl. Fusion **45** (2005) S86-S97

Luce T. C., Fusion Science and Technology **48** (2005) 1212

Maggi C. F. et al., Nucl. Fusion **47** No 7 (July 2007) 535-551

Mailloux J. et al., 1997 J. Nucl. Mater. **241-243** 745

Maraschek M. et al., *Nucl. Fusion* **45** No 11 (November 2005) 1369-1376

Mazon D. et al., *Plasma Phys. Control. Fusion* **45** No 7 (July 2003) L47-L54

McDonald D. C. et al., *Plasma Phys. Control. Fusion* **46** No 5A (May 2004) A215-A225

McDonald D.C. et al., Nucl. Fusion **47** (2007) 147-174

Mikkelsen D. R., Phys. Fluids B **1** (2) 1989, 333

Moreau D. et al., 21st Fusion Energy Conference, 16-21 October 2006, Chengdu, China, EX/P1-2

Murakami et al., *Phys of Plasma* **13** (2006) 056106
Neu R. Phys. Scr. 2006 No T123 (April 2006) 33-44
Oikawa T. et al., 5th IAEA Technical Meeting on steady state operations of magnetic fusion devices, May 2007, Daejeon, Korea, O-IT-2
Oikawa T. et al., *Nuc. Fus.* **40** (2000) 1125
Okabayashi M. et al., *Nuc. Fusion* **45** (2005) 1715-1731
Oyama N. et al., 21st Fusion Energy Conference, 16-21 October 2006, Chengdu, China, EX/1-3
Peeters A. G. *Plasma Phys. Control Fusion* **42** (2000) B231-B242
Petty C. C. et al., *Phys. Plasma* **5** (1998) 1695
Politzer P.A. et al 2005 *Nucl. Fusion* **45** 417-424
Prater R.. et al., 21st Fusion Energy Conference, 16-21 October 2006, Chengdu, China, EX/4-2
Sakamoto Y. et al., 21st Fusion Energy Conference, 16-21 October 2006, Chengdu, China, EX/P1-10
Sauter O. et al., *Phys. Rev. Letter* **84** 105002-1
Shinohara K. Et al., *Plasma Phys. Control. Fusion* **46** No 7 (July 2004) S31-S45
Sips A. C. C. et al., 21st Fusion Energy Conference, 16-21 October 2006, Chengdu, China, EX/1-1, submitted to *Nuc. Fus.* 2007.
Sips A. C. C. et al., *Plasma Phys. Control. Fusion* **47** (2005) A19-A40
Sips A. C. C. et al., *Plasma Phys. Control. Fusion* **44** (2002) B69-B83
Staebler et al., et al., *Nucl. Fusion* **45** (2005) 617-625
Stangeby P C *Nuc. Fus.* **33** (1993) 1695
Strait E. J. et al., *Strait E. J. Physics of Plasmas* **14**, 056101 (2007)
Suzuki T. et al., , 21st Fusion Energy Conference, 16-21 October 2006, Chengdu, China, EX/6-4
Takase Y. et al., 21st Fusion Energy Conference, 16-21 October 2006, Chengdu, China, EX/1-4
Takenaga H. et al., *Nucl. Fusion* **43** (2003) 1235-1245
Takenaga T. and JT-60U team, 21st Fusion Energy Conference, 16-21 October 2006, Chengdu, China, OV-2
Takenaga T. et al., *Nucl. Fusion* **45** No 12 (December 2005) 1618-1627
Tala T. et al., *Nucl. Fusion* **45** No 9 (September 2005) 1027-1038
Terry P. W., 2000 *Rev. Mod. Phys.* **72** 109
Testa D. et al., 29th *Plasma Phys. Control. Fusion* **46** (2004), S59-S79.
Turnbull A. D. et al., *Nuc. Fus.* **38** (1998) 1467
Vermare L. et al., *Nucl. Fusion* **47** (2007) 490-497
Villone F. et al., 2007 this conference.
Vlad G., et al., *Nucl. Fusion* **46** (2006) 1-16
Wade M. D. and DIII-D team, 21st Fusion Energy Conference, 16-21 October 2006, Chengdu, China, OV-4
Wade M. D. et al., *Nucl. Fusion* **45** (2005) 407-416
Wagner F. et al., *Phys. Rev. Letter* **53** (1984) 1453-1456

Wakatani et al., *Plasma Phys. Control. Fusion* **40** (1998) 597
Weiland J 2000 *Collective Modes in Inhomogeneous Plasmas* (Bristol: Institute of Physics Publishing)
Wilson H. R. et al., *Nuc. Fusion* **32** (1992) 257
Wolf R. C. et al., Plasma Phys. Control. Fusion **43** No 9 (September 2001) 1239-1254
Wolf R. C. et al., *Plasma Phys. Control. Fusion* **45** (2003) R1-R91
Zonca F. et al., *Physics of Plasmas* **9** (2002) 4939

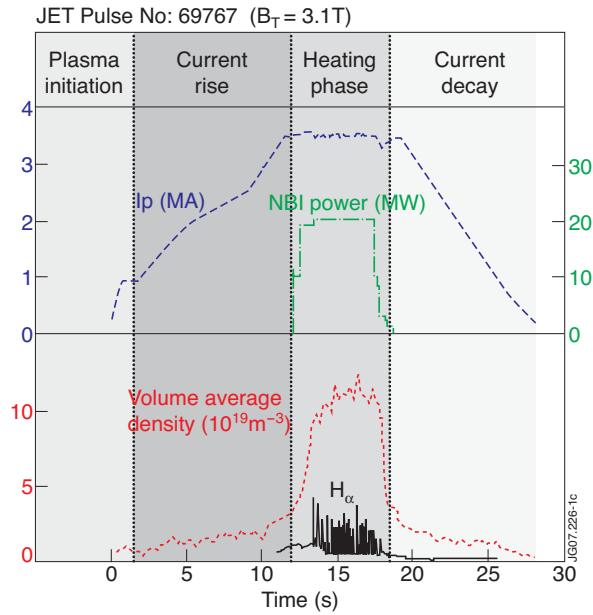


Figure 1: Example of a non-inductive H-mode run at JET with a plasma current of 3.5MA and a magnetic field strength of 3.1T. The various phases of the scenario are indicated on the figure. In this JET discharge, the heating is provided by Neutral Beam Injection (NBI). As the power is injected, the H-mode is produced and characterised by a transition to a higher confinement state produced by presence of a layer of reduced transport at the plasma edge accompanied by strong spikes on the H_α emission. This type of discharge would be run in ITER for typically 400s and produce a fusion power of 500MW.

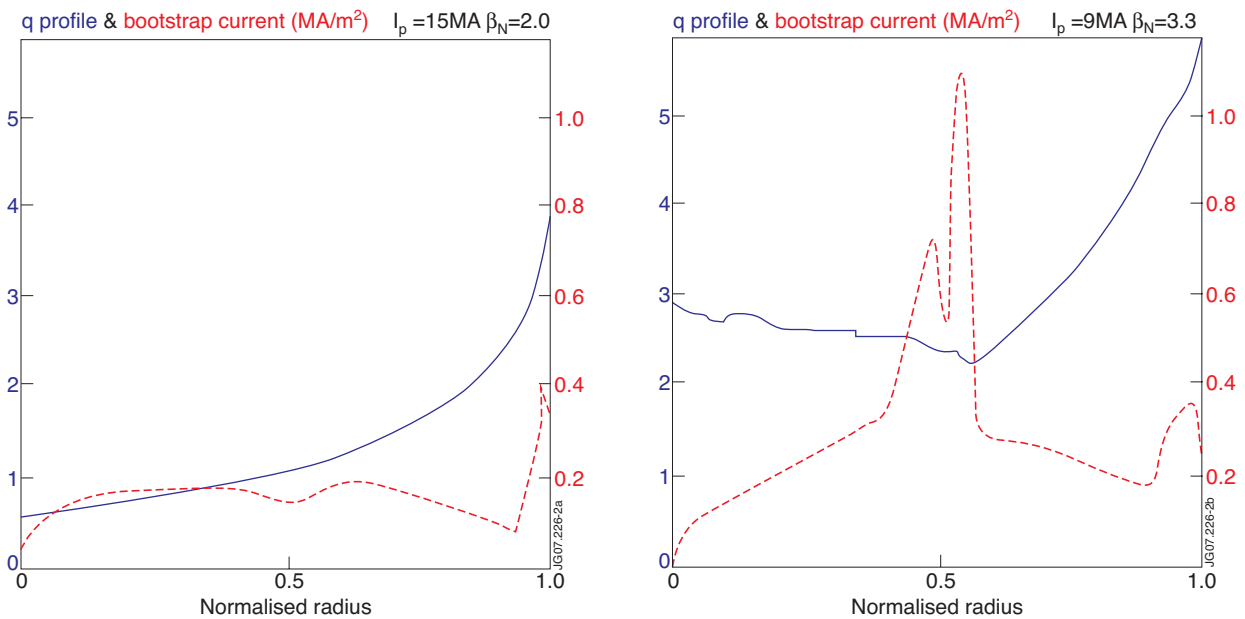


Figure 2: ITER simulation from the CRONOS [Basiuk 2003] code showing the role of the bootstrap current on the q profile as β_N is increased and q_{95} decreased. The bootstrap current can alter significantly the q profile shape and modify the transport and stability property of the discharge.

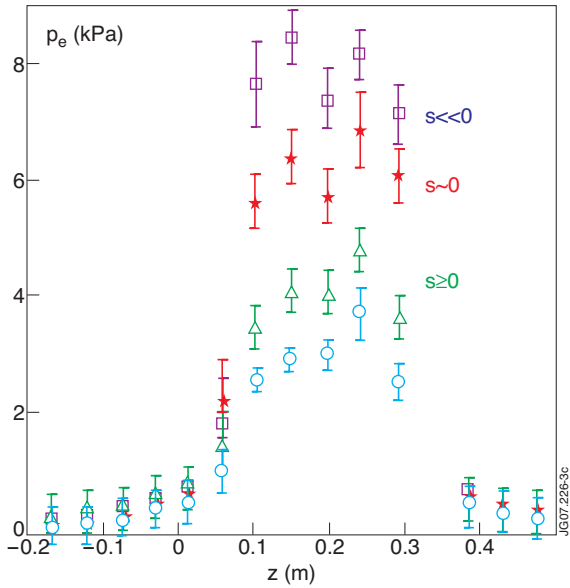


Figure 3: Sharp increase of the electron pressure when the magnetic shear is being varied from slightly positive, to zero and then strongly negative. This experiment carried out in the TCV tokamak illustrates the effect of the magnetic shear on the formation of internal transport barriers [Sauter 2006].

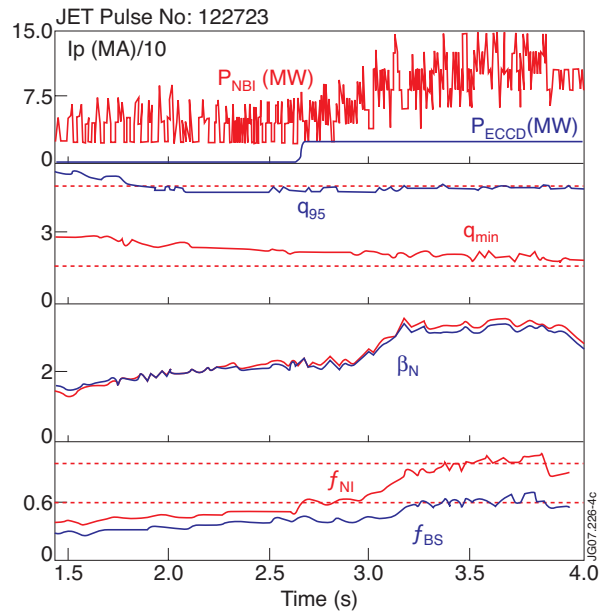


Figure 4: Typical steady state scenario run in the DIII-D tokamak. This scenario meets simultaneously the ITER steady state normalised targets indicated by horizontal dashed lines. In this scenario, 60% of the total current is driven by the bootstrap current and the remainder is delivered by EC and NB current drive. The q profile is broad and weakly reversed with $q_{min}=1.7$ located at $r/a \sim 0.6$. From [Murakami 2006].

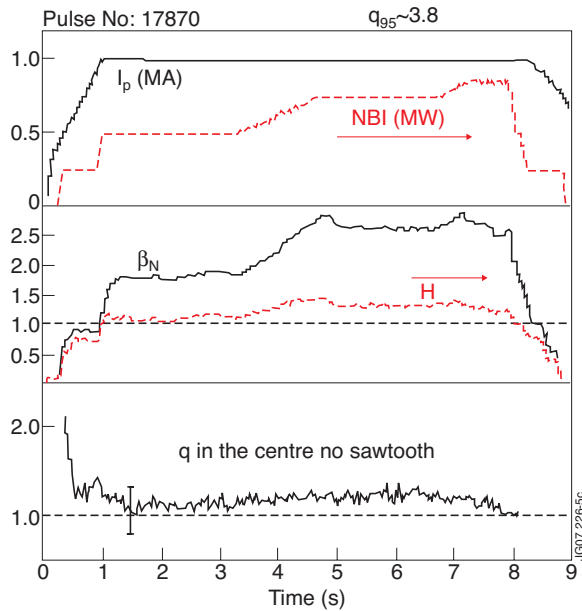


Figure 5: Typical stationary hybrid scenario achieved in ASDEX Upgrade. In this scenario, almost 35% of the total current is driven by the bootstrap current and 25% by NB current drive. The q profile is kept above unity for the duration of the pulse with an improved H factor of 1.3-1.4 during the high power phase. [Staeblner 2005].

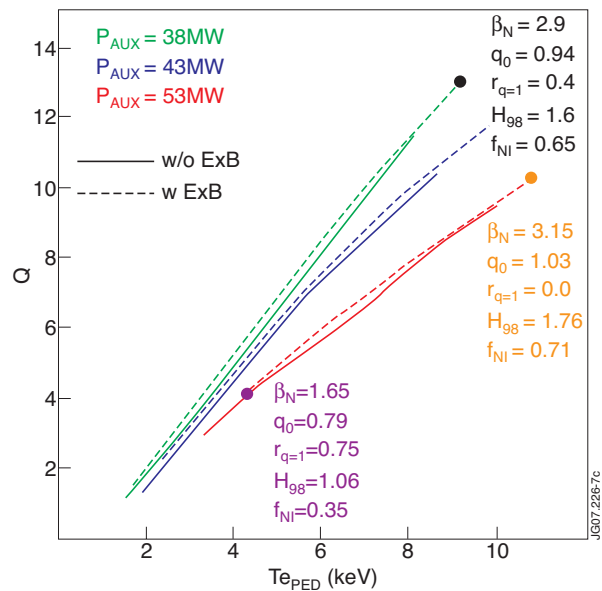


Figure 6: β_N versus ρ^* parameter space showing the coverage of the DB3 H-mode database used to derive the IPB98(y,2) scaling law [McDonald 2007]. Note that the database has very poor coverage at high normalised pressure, making the extrapolation of the advanced tokamak scenario confinement to ITER more uncertain than for the standard H-mode.

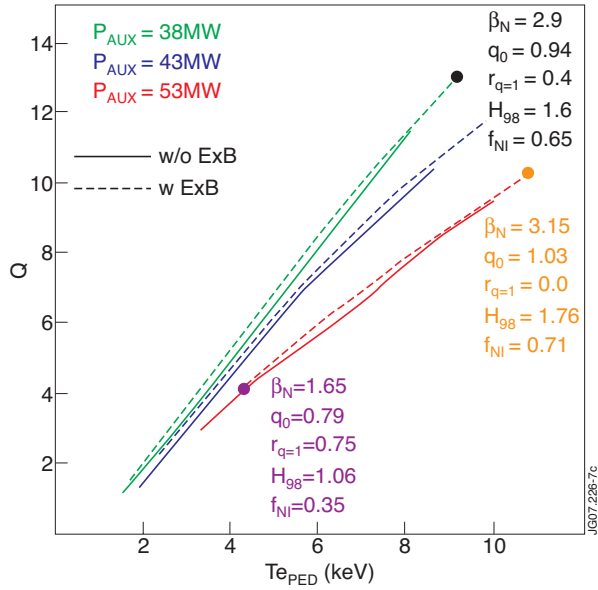


Figure 7: Dependence of the fusion gain factor with the pedestal temperature as given by the simulation with the GLF23 transport code from [Kessel 2005]. Dashed lines refer to the same calculation with the inclusion of the ExB shearing rate stabilisation. Note the differences on the total non-inductive current (f_{NI}), central q values (q_0) and radius of the $q=1$ surface ($r_{q=1}$) for the three points indicated on the graph. The H-mode edge pedestal (such as the temperature value) has a large impact on the current profile evolution modelling for advanced tokamak scenario.

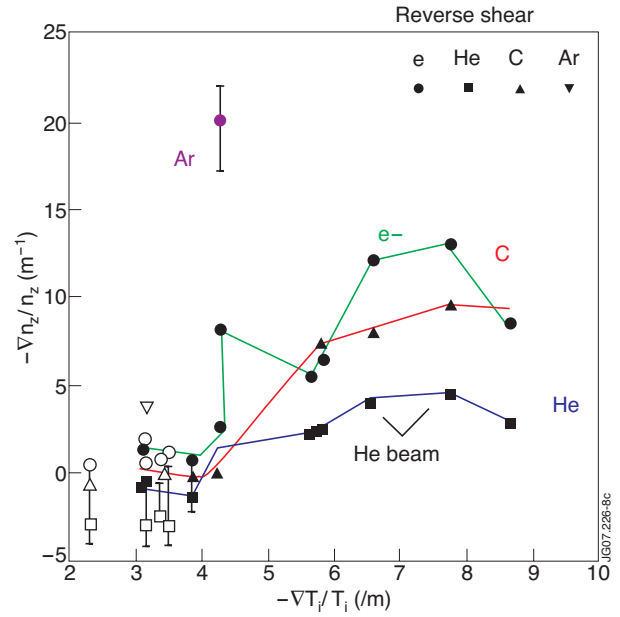


Figure 8: Dependence of impurity density gradient (for Argon in purple, Carbon in red and Helium in blue and electronic density in green) with the ion temperature gradient in reversed shear discharges with internal transport barrier. From [Takenaga 2005]

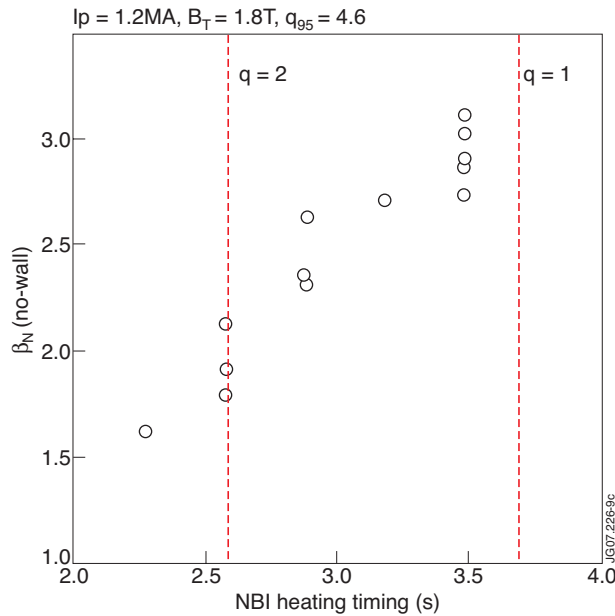


Figure 9: Dependence of the normalised pressure at the no-wall limit with the neutral beam heating time in JET. The no-wall β_N is determined by MHD spectroscopy: the plasma response to an oscillating magnetic perturbation in the error field coils is recorded as the plasma pressure is increased. The neutral beam timing is a signature of the minimum value of q : as the NBI timing is advanced in the current ramp up, the current density profile penetration is stopped higher in q values by the temperature increase. The two vertical lines approximately indicate the observation time of the $q=2$ and $q=1$ surface from MHD analysis. This illustrates the sensitivity of the no-wall limit with the q profile shape [Gryaznevitch 2007].

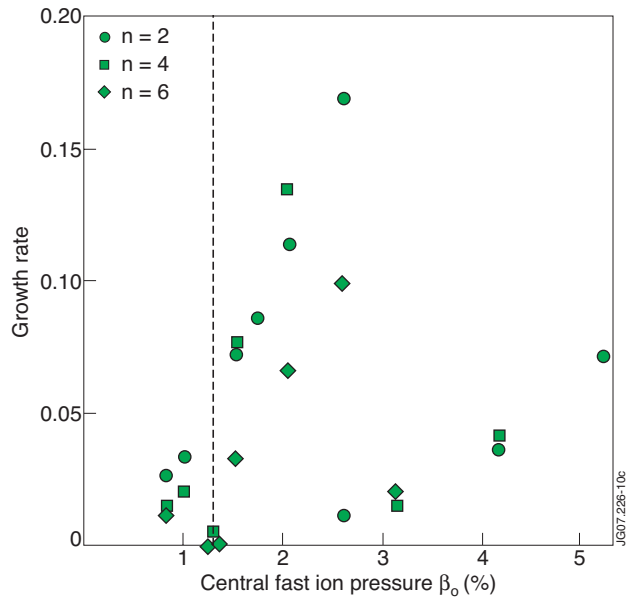


Figure 10: Growth rate of Alfvénic modes ($n=2$: circles; $n=4$ squares; $n=6$ diamond) for the steady state scenario (in green) and for the hybrid stationary scenario (in blue) as function of the central fast ion pressure normalised to the pressure of the hybrid scenario. This computation suggests that the Alfvénic modes are more unstable for q profiles with $q_{min} > 2$ (steady state scenario) than for q profiles close to unity in the plasma core (hybrid scenario). [Vlad 2006].

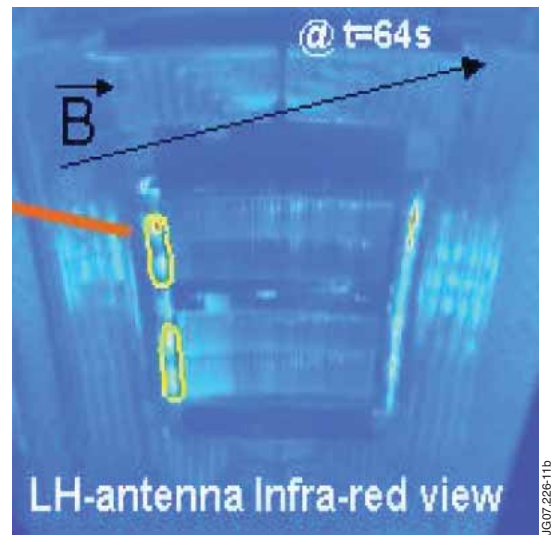
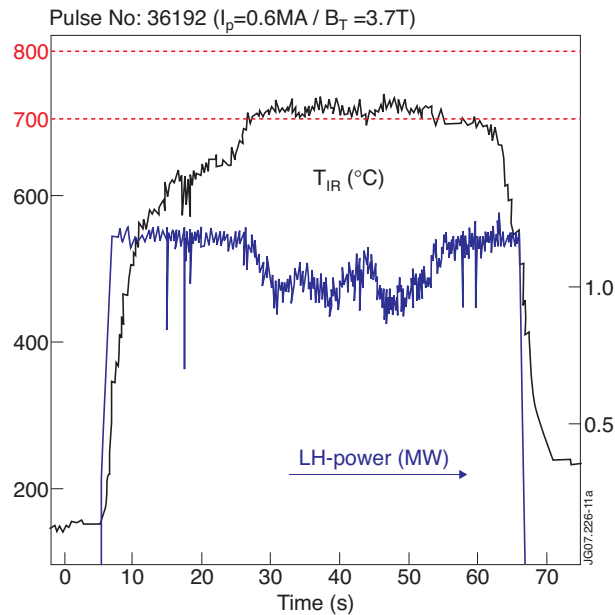


Figure 11: Example of the control of transient power load on an LH-launcher in Tore Supra. As the temperature in the indicated mask on the infra-red picture exceeds 950 deg, the control system starts to limit the power launched by the antenna. The temperature increase is caused by fast electrons accelerated by the high electric fields in the vicinity of the launcher mouth. This protective action is executed in combination with the control of the LH-deposition profile [Joffrin 2006].